coatings

MDPI

Review

Effect of Pre-Heat-Treatment on the Oxidation Resistance of MCrAlY Coatings: A Review

Bangyan Zhang *, Shijie Zheng, Jiajian Dong, Weiwei Yin, Hongbin Wu, Lixi Tian and Guangming Liu

Key Laboratory for Microstructural Control of Metallic Materials of Jiangxi Province, School of Materials Science and Engineering, Nanchang Hangkong University, Nanchang 330063, China; 2101085600026@stu.nchu.edu.cn (S.Z.); 2101080501003@stu.nchu.edu.cn (J.D.); 2201085600087@stu.nchu.edu.cn (W.Y.); 2001085600154@stu.nchu.edu.cn (H.W.); 70682@nchu.edu.cn (L.T.); gemliu@126.com (G.L.)

* Correspondence: zby@nchu.edu.cn

Abstract: High-performance gas turbines and aircraft engines necessitate MCrAlY (M = Ni, Co, or Ni/Co) coatings with exceptional oxidation resistance. Pre-heat-treatment can enhance the performance of MCrAlY bond coatings in the following ways: First, it reduces the porosity of the bond coating and promotes the diffusion of elements within it. Second, pre-heat-treatment allows for the formation of a continuous, dense, and moderately thick layer of pure Al_2O_3 scale, which helps to delay the formation of mixed oxides. Lastly, proper pre-heat-treatment can increase the grain size of the Al_2O_3 scale, leading to a lower growth rate of the oxide scale. Additionally, this article proposes new directions for developing more reasonable and effective pre-heat-treatment methods, laying the foundation for the creation of thermal barrier coatings (TBCs) with greater durability and higher performance.

Keywords: thermal barrier coatings; MCrAlY coating; thermally grown oxides; pre-treatment; oxidation resistance

Citation: Zhang, B.; Zheng, S.; Dong, J.; Yin, W.; Wu, H.; Tian, L.; Liu, G. Effect of Pre-Heat-Treatment on the Oxidation Resistance of MCrAlY Coatings: A Review. *Coatings* **2023**, *13*, 1222. https://doi.org/10.3390/coatings13071222

Academic Editor: Alessandro Latini

Received: 12 June 2023
Revised: 30 June 2023
Accepted: 6 July 2023
Published: 8 July 2023

1. Introduction

To enhance the efficiency and power output of gas turbines, it is necessary to steadily augment the temperature of the inlet gas fueling the turbine. As a result, the requirements for high-temperature resistance materials utilized in hot-end components are becoming increasingly stringent [1–6]. Film cooling technology and thermal barrier coatings (TBCs) have become the principal methods for guaranteeing that blades operating at high temperatures (ranging from 1100 °C to 1900 °C) conform to service requirements. TBCs primarily act as heat-insulating and anti-oxidation agents, effectively shielding superalloy substrates from damaging effects [7–12].

Typically, TBCs consist of a ceramic layer, MCrAlY bond coat, and a thermally-grown oxide (TGO) scale produced on the bond coat surface during high-temperature service [13–26], as depicted in Figure 1. The ceramic layer, with its low thermal conductivity, primarily functions as a heat insulator [11,27–29]. The bond coat supplies the required elements for TGO growth and reduces the thermal mismatch between the ceramic layer and the superalloy matrix [30,31]. A continuous and dense TGO can hinder the inward migration of external oxygen, thus minimizing the oxidation rate of the coatings.

The growth of TGO is one of the key factors leading to a spalling failure of the ceramic layer. TGO is usually composed of one or more oxides, such as α-Al_2O_3, NiO, Cr_2O_3 and (Ni, Co)(Cr, Al)$_2O_4$. Among them, NiO, Cr_2O_3 and (Ni, Co)(Cr, Al)$_2O_4$ are collectively referred to as mixed oxides. To achieve the objectives of anti-oxidation and to delay spallation of the ceramic layer in TBC's system, it is necessary to have a continuous, dense and slow-growing TGO. Studies have shown that the rapid growth of mixed oxides can result in a rapid increase in the local growth stress in the neighboring ceramic layer, causing

local cracking and peeling of the ceramic layer [32–34]. α-Al_2O_3 is considered an ideal TGO constituent because of its excellent high temperature stability, low ion diffusion rate, and high compactness. Multiple studies have demonstrated that when the thickness of TGO reaches a critical threshold of 5–10 µm, it causes cracks to form in the ceramic layer, leading to the failure of TBCs [35–38]. Thus, it is critical to prevent the formation of mixed oxides and achieve the formation of a dense and continuous TGO composed only of pure α-Al_2O_3 with a specific thickness and a slow growth rate. This can help to reduce the stress in the nearby ceramic layer and prolong the lifetime and performance of TBCs.

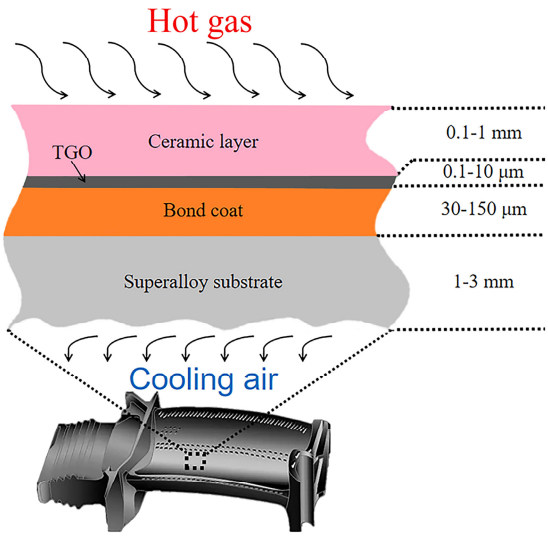

Figure 1. Schematic diagram of thermal barrier coatings (TBCs) structure.

Research reports suggest that appropriate pre-heat-treatment of the bond coat before its use can significantly inhibit the formation of mixed oxides and reduce the TGO growth rate, thus prolonging the service life of TBCs [39–43]. Pre-heat-treatment is an inexpensive, simple to operate, and highly effective method for TBC protection. Therefore, it is crucial to elucidate relevant research reports on this method to further increase its utilization in the industry and extend the life of TBCs.

This article explores the impact of MCrAlY bond coats and TGO on the lifespan of TBCs. Furthermore, it highlights the effects of pre-heat-treatment on the bond coat structure and delves into the underlying mechanisms by which pre-heat-treatment enhances high-temperature oxidation resistance. Ultimately, this article identifies avenues for the development of TBCs with high reliability and longevity.

2. Brief Introduction to MCrAlY Coatings

Various deposition techniques, such as high-velocity oxygen fuel (HVOF) spraying, low-pressure plasma spraying (LPPS), electron beam-physical vapor deposition (EB-PVD), and others, are commonly employed for the fabrication of MCrAlY bond coat.

In the HVOF process, the combustion of fuel gas and oxygen generates a high-speed jet flame that melts and accelerates the MCrAlY powder particles onto the substrate in the air. The intense jetting force leads to rapid particle deformation and quick cooling, resulting in the solidification and formation of a coating [44]. The HVOF MCrAlY bond coat exhibits high oxygen content, low density, and high residual stresses, which could potentially result in negative consequences [45]. During the LPPS process, MCrAlY powder is heated and accelerated by the high-speed plasma flame in a low-pressure protective atmosphere, resulting in the deposition of a tightly compacted coating on the substrate surface. The LPPS bond coat exhibits a lower oxygen content and a comparatively denser microstructure compared to the HVOF MCrAlY coating [46]. In the EB-PVD process, the MCrAlY alloy material is evaporated and deposited onto the substrate surface using an electron beam in a vacuum environment. The evaporated MCrAlY material is

accelerated and cooled, forming a dense coating on the substrate [47]. EB-PVD MCrAlY bond coats exhibit low oxygen content, high chemical homogeneity, and excellent high-temperature stability [48]. However, compared to LPPS, the production cost of EB-PVD is typically higher.

The failure of MCrAlY bond coats is predominantly attributed to high-temperature oxidation. During the oxidation process, the aluminum element is consumed, resulting in alterations to the distribution of internal elements and even to the composition of phases within the bond coat, ultimately leading to failure. In order to improve the high-temperature oxidation resistance of the bond coat, various methods can be utilized, such as alloying, alitizing, and pre-heat-treatment. Among these methods, pre-heat-treatment is particularly beneficial in reducing the porosity of the bond coat, leading to a more uniform distribution of internal elements, and resulting in a high-quality protective oxide scale on the coatings. This will effectively delay the failure of the bond coat exposed to a high-temperature atmosphere. Notably, pre-heat-treatment is both cost-effective and simple to implement, making it a highly worthwhile approach to consider.

3. The Effect of the MCrAlY Coating Microstructure on Its High Temperature Oxidation Resistance

The MCrAlY bond coat is made up of a multifaceted alloy, where a considerable portion of the aluminum is dispersed in the matrix phase as β-NiAl intermetallic compound phase, while most of the chromium element is present in the γ-Ni solid solution phase. A higher relative content of the β phase in the coating is beneficial to improve the anti-oxidation performance of the bond coat. Conversely, increasing the relative content of the γ phase enhances the hot corrosion resistance of the bond coat. A sufficient Al content in the bond coat can ensure selective oxidation to form a stable and continuous Al_2O_3 scale [49,50]. However, it should be noted that the presence of Al also reduces the toughness and mechanical properties of the coatings. Therefore, under the premise of ensuring that the coating has a certain anti-oxidation performance, the Al content should be reduced as much as possible. The addition of an optimal amount of Cr to the coating can facilitate the formation of the Al_2O_3 scale while minimizing the required Al content. This is due to the fact that the presence of Cr can produce a protective chromia (Cr_2O_3) scale, which reduces the burden on the Al_2O_3 scale and enables its efficient growth without requiring high Al content. Furthermore, the optimal incorporation of Y element into the bond coat can significantly enhance the bonding strength between the TGO and the bond coat [51,52].

The level of oxygen content present in the MCrAlY bond coat has a significant impact on its high-temperature oxidation resistance [53]. A higher oxygen content in the bond coat leads to a reduced aluminum content within the coating, thus adversely affecting the coating's oxidation resistance. For instance, due to the higher oxygen content in the bond coat created using atmospheric plasma spraying (APS) as compared to the coating produced using LPPS, the TGO on the surface of the APS bond coat grows at a faster rate than that of the latter.

The density of the MCrAlY bond coat is a critical factor that affects its oxidation resistance at elevated temperatures. Porosity and cracks present within the bond coat can clog the diffusion of elements within the coating. In addition, the oxidizing gases such as O_2 present within these defects can trigger a selective oxidation reaction with the coating when exposed to high temperatures, leading to the formation of internal oxides. This can cause an insufficient level of aluminum to be retained within the coating and result in the early formation of mixed oxides on the coating surface.

4. The Effect of TGO Growth Behavior on the High Temperature Oxidation Resistance of MCrAlY Bond Coats

The microstructure of the TGO plays a crucial role in determining the bond coat's ability to resist oxidation at high temperatures. TGO that is composed purely of α-Al_2O_3 demonstrates optimum service performance and is acknowledged as the desired TGO composition. However, TGO usually contains other quasi-stable Al_2O_3 phases, such as

γ-Al_2O_3 or θ-Al_2O_3, with needle-like or sheet-like morphologies [54–57]. Reports [56,58–61] suggest that the growth rate of these quasi-stable Al_2O_3 phases is more than twice as high as that of dense α-Al_2O_3. Cr_2O_3 exhibits anti-oxidation and anti-corrosion protection effects at temperatures below 900 °C. However, when the ambient temperature exceeds 900 °C, Cr evaporation is likely to occur [62]. Maier et al. [63] reported that the growth rate of NiO is three times higher than that of α-Al_2O_3. (Ni, Co)(Cr, Al)$_2O_4$ is a composite spinel-like oxide whose growth is usually accompanied by local rapid volume expansion [64], resulting in a porous structure. Reports [65,66] suggest that the mixed oxides mentioned above can cause significant growth stress in the adjacent ceramic layer, thus accelerating the cracking of the ceramic layer (Figure 2). Additionally, the researchers performed thermal cycling experiments on bond coats with varying ratios of mixed oxides enveloping their surfaces. The samples were subjected to a temperature of 1150 °C for 27 min and then rapidly cooled to room temperature within 4 min, completing one thermal cycle. The thermal cycling life was defined as the number of thermal cycles required for 50% peeling of the ceramic top coating from the bond coat. It can be observed that as the coverage of mixed oxides on the surface increased, the ceramic layer became more prone to cracking, resulting in a significant decrease in the thermal cycling life of TBCs (Figure 3). Hence, inhibiting the formation of mixed oxides and forming a dense and continuous TGO layer with a specific thickness of pure α-Al_2O_3 holds great significance for enhancing the service life of TBCs.

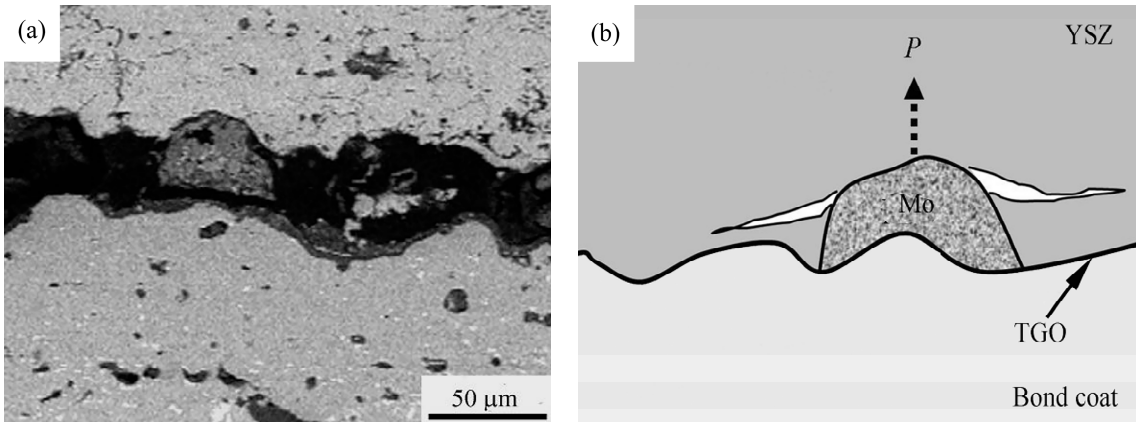

Figure 2. Effect of mixed oxides on the cracking of ceramic coating. (**a**) Typical fracture morphology of coating. (**b**) schematic diagram of cracking mechanism [65]. Copyright 2009, Springer Nature.

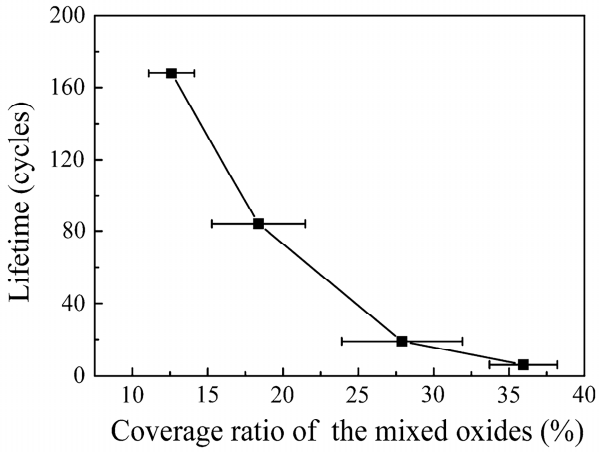

Figure 3. Correlation between the coverage of mixed oxides on the bond coat's surface and the lifespan of TBCs. (Coverage ratio is defined as the ratio of the areas covered by the mixed oxides on the bond coat of the failed TBCs to the total areas of the oxides in the spallation areas) [65]. Copyright 2009, Springer Nature.

The thickening of TGO is a significant source of stress that can cause TBCs to crack and eventually fail [19,67–71]. During high-temperature service, an increase of the TGO thickness can generate high growth stress in the nearby ceramic layer, and the greater the thickness of TGO, the higher the magnitude of the growth stress [67,72]. Once the thickness of TGO reaches a critical value, the ceramic layer will begin to peel off and finally fail [67,68,73]. Dong et al. [67] deposited a layer of yttria-stabilized zirconia (YSZ) onto the surface of a NiCoCrAlTaY bond coat with different initial TGO thicknesses. Subsequently, thermal cycling tests were conducted on the TBCs using a gas burner test setup, with heating, holding, and cooling durations of 70, 50, and 120 s respectively. The thermal cycle life of TBCs was defined as the number of cycles that the YSZ layer endured before cracking. The results of the experiment indicated a significant reduction in the thermal cycle life of TBCs as the initial TGO thickness of the bond coat increased (Figure 4). As a result, inhibiting the TGO growth rate and enhancing the oxidation resistance of the bond coat are crucial to prolonging the life of TBCs. In a previous study by the authors of this paper [39], it was found that the grain size of TGO plays a crucial role in its growth rate. TGO with larger grains has a slower growth rate and enhanced high-temperature oxidation resistance. These findings have significant implications for the development of long-life TBCs.

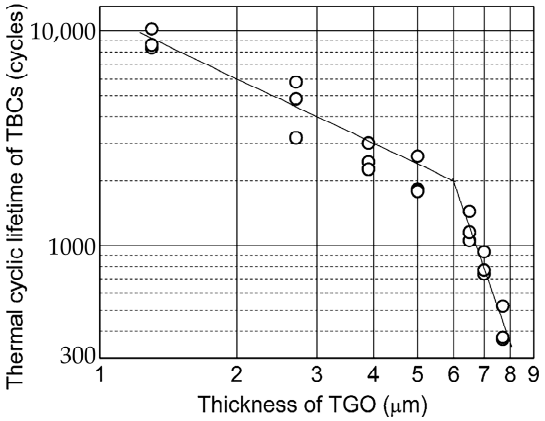

Figure 4. Relationship between the oxide scale (TGO) thickness and thermal cycle life of TBCs [67]. Copyright 2014, John Wiley and Sons.

5. The Effect of Pre-Heat-Treatment on the Bond Coat Structure

Pre-heat-treatment has the ability to influence the ratio of β phase to γ phase in the bond coat, thus regulating the distribution of elements and enhancing the coating density. This adjustment facilitates the formation of a stable and continuous Al_2O_3 scale during the initial stages of high-temperature oxidation, while inhibiting the formation of mixed oxides, ultimately improving the high-temperature oxidation resistance of the bond coat.

Saeidi et al. [74] produced a CoNiCrAlY bond coat using two spray techniques: HVOF and vacuum plasma spraying (VPS). The as-sprayed HVOF bond coat had a γ/β structure similar to the original powder, whereas the as-sprayed VPS bond coat had a single γ phase. Both types of bond coat were subjected to a vacuum pre-heat-treatment at 1100 °C for 3 h. The results showed that the vacuum pre-heat-treatment transformed the structure of the VPS bond coat from a single γ phase to a γ/β two-phase structure, and coarsened the β phase structure in the HVOF bond coat. Furthermore, vacuum pre-heat-treatment reduced the porosity in the bond coat and improved its compactness to a certain extent.

Ullah et al. [75] fabricated a NiCoCrAlY bond coat on a nickel-based single crystal superalloy via arc ion plating, subsequently subjecting the bond coat to a vacuum pre-heat-treatment at 1000 °C for 4 h ($pO_2 < 6 \times 10^{-3}$ Pa). Figure 5 shows the surface morphology, cross-sectional morphology, and X-Ray diffraction results of the as-deposited and pre-treated bond coat. From the figure, it can be observed that the vacuum pre-heat-treatment had no significant effects on the bond coat surface morphology. The vacuum pre-heat-treatment healed the original pores in the bond coat and improved the coating density.

The as-deposited bond coat was primarily composed of γ/γ' matrix phase; however, the vacuum pre-heat-treatment precipitated the β-(Ni, Co)Al phase (the dark phase in the coating in Figure 6e) in the γ/γ' matrix phase.

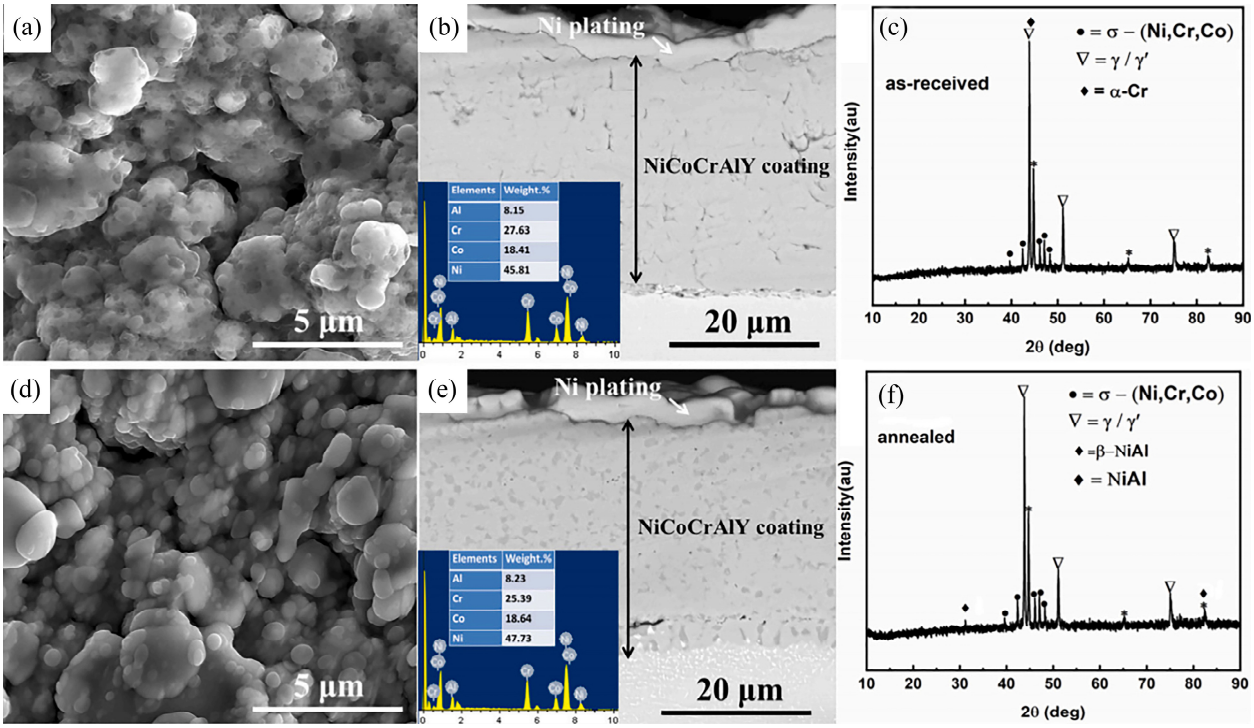

Figure 5. (**a**) Surface and (**b**) cross-sectional morphologies, (**c**) XRD results of the as-deposited NiCoCrAlY bond coat, (**d**) surface and (**e**) cross-sectional morphologies, (**f**) XRD results of the pre-treated NiCoCrAlY bond coat [75]. Copyright 2020, Elsevier.

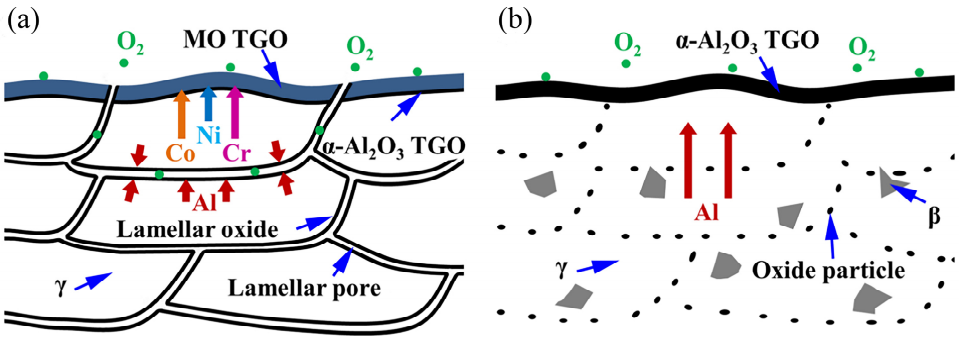

Figure 6. Schematic diagram depicting the microstructural changes of atmospheric plasma spraying (APS) CoNiCrAlY bond coat during the pre-heat-treatment process. (**a**) As-sprayed bond coat, (**b**) pre-treated bond coat [43]. Copyright 2018, Elsevier.

Meng et al. [43] investigated the impact of a controlled atmosphere pre-heat-treatment (10 h at 1100 °C, $pO_2 < 1 \times 10^{-3}$ Pa) on the microstructure of the APS CoNiCrAlY coating. Due to the nature of the preparation process, there are numerous pores inside the as-sprayed coating, and a continuous initial internal oxide scale can be observed on the inner walls of these pores, which obstructs the diffusion of elements in the coating and results in the pre-generation of mixed oxides (Figure 6a). The pre-treated coating structure, as shown in Figure 6b, revealed that the pores inside the coating had been healed, and the initial oxide scale had broken into discontinuous oxide particles that are conducive to the rapid migration of elements in the coating during subsequent high-temperature oxidation processes to suppress the formation of mixed oxides.

6. The Effect of Pre-Heat-Treatment on the TGO Growth Behavior

The microstructure of the TGO on the bond coat surface is directly affected by high-temperature pre-treatment. Suitable pre-heat-treatment can result in the formation of a layer of uniform, continuous and dense pure α-Al_2O_3 TGO with a specific thickness on the bond coat surface, which can effectively inhibit the formation of mixed oxides and the growth rate of the TGO [76–79].

Saeidi et al. [74] fabricated a CoNiCrAlY bond coat using VPS and HVOF methods respectively, and then pre-treated the coatings with low oxygen partial pressure at 1100 °C for 3 h. After isothermal oxidation at 1100 °C for 100 h, the surface of the bond coat without pre-heat-treatment featured double-layer TGO with an inner layer of alumina and an outer layer of mixed oxide. In contrast, the surface of the bond coat with pre-heat-treatment had only pure Al_2O_3 TGO.

Xie et al. [80] carried out a low oxygen partial pressure pre-heat-treatment ($pO_2 < 10^{-3}$ Pa) of the cold sprayed NiCoCrAlY bond coat at 1050 °C for 4 h. This resulted in the formation of a uniform and continuous α-Al_2O_3 scale with a thickness of 0.47 ± 0.02 μm on the coating surface. After high-temperature oxidation in air at 1050 °C for 400 h of both as-prepared and pre-treated bonded coats, the α-Al_2O_3 grain size on the surface of the pre-treated bond coat was almost twice as large as that of the bond coat without pre-heat-treatment.

Meng et al. [42] carried out a pre-heat-treatment under low oxygen pressure ($pO_2 < 10^{-9}$ Pa) on a LPPS CoNiCrAlY bond coat at 1100 °C for 4 h. Then, both with and without heat treatment (W/HT and W/O HT) were subjected to high-temperature oxidation at 1050 °C for 4, 25, 64, 100 and 200 h. Figure 7 presents the cross-sectional microstructure of the TGO layer. It can be observed that the low oxygen pressure pre-heat-treatment could inhibit the formation of mixed oxides and bring down the growth rate of the α-Al_2O_3 scale. By observing the α-Al_2O_3 grain size at the interface between the CoNiCrAlY bond coat and TGO layer in Figure 8, it is notable that the low oxygen pressure pre-heat-treatment promotes the growth of the α-Al_2O_3 grains, which decreased the diffusion rate of ions within the oxide scale, thereby inhibiting the α-Al_2O_3 scale growth.

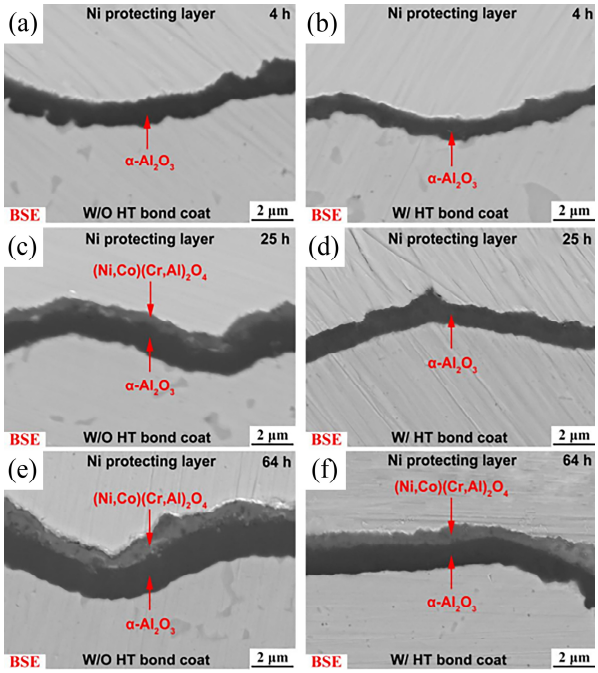

Figure 7. The TGO cross-sectional microstructure of low-pressure plasma spraying (LPPS) CoNiCrAlY bond coat without and with the pre-heat-treatment (W/O HT and W/HT) and high-temperature oxidation at 1050 °C with different times. (**a**,**c**,**e**) W/O HT bond coat; (**b**,**d**,**f**) W/HT bond coat [42]. Copyright 2019, Elsevier.

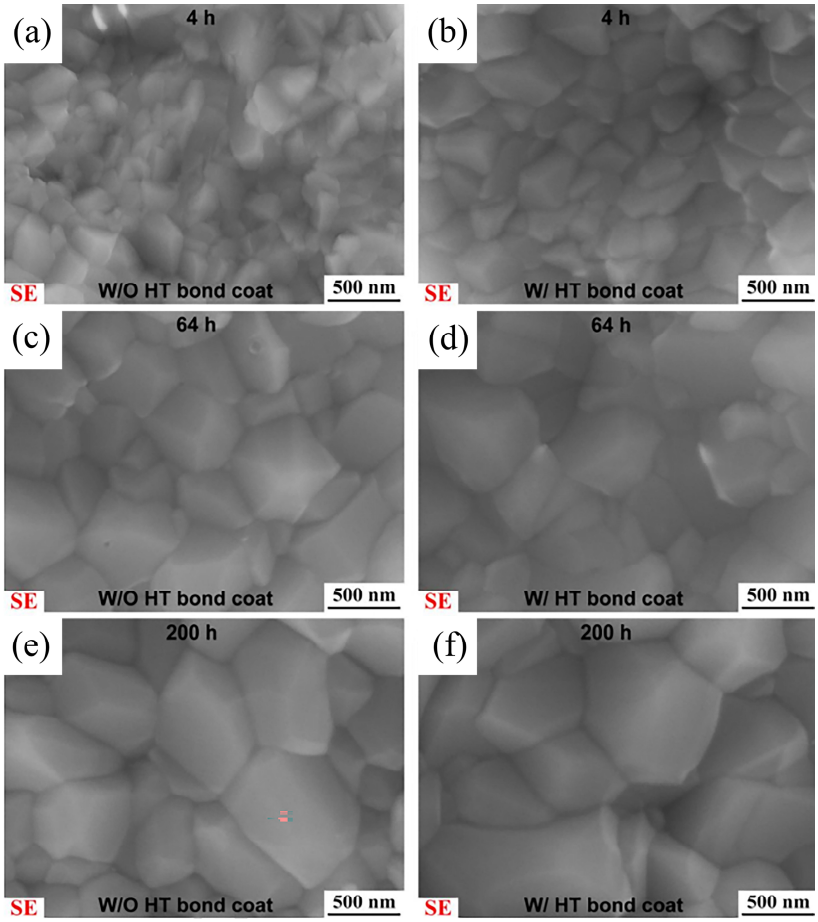

Figure 8. The grain size of α-Al_2O_3, which is adjacent to the interface between the TGO layer and CoNiCrAlY bond coat, after varying high-temperature oxidation times at 1050 °C in air. (**a**,**c**,**e**) W/O HT bond coat; (**b**,**d**,**f**) W/HT bond coat [42]. Copyright 2019, Elsevier.

Zhang et al. [81] fabricated a CoNiCrAlY bond coat using LPPS and observed that the weak bond between the coating and the splash particles on the coating surface resulted in the early formation of mixed oxides. A two-step pre-heat-treatment solution was proposed, that is, pre-diffusion (3 h at 1150 °C, $pO_2 < 2 \times 10^{-3}$ Pa) and then pre-oxidation (4 h at 1000 °C + 4 h at 1080 °C, $pO_2 < 3$ Pa). The obtained outcomes indicate that, following the two-step pre-heat-treatment, the previously weak interface between the splash particle and coating had been powerfully reinforced, and the formation of mixed oxides had been effectively inhibited during the subsequent long-term isothermal oxidation (at 1000 °C in air).

Based on the above analysis, it is evident that the pre-heat-treatment process plays a crucial role in the structure and growth behavior of TGO. Consequently, with an appropriate pre-heat-treatment, the high temperature oxidation resistance of the bond coat can be promoted effectively. Thus, it becomes vital to systematically investigate the influence of different technologies in pre-heat-treatment (such as temperature, time, oxygen partial pressure in the atmosphere, etc.) on the growth behavior of TGO.

6.1. The Effect of Pre-Heat-Treatment Temperature and Time on Growth Behavior of TGO

Lih et al. [82] used VPS to manufacture a NiCrAlY bond coat. The as-sprayed coatings were pre-oxidized at varying temperatures and times. Following pre-heat-treatment, a ZrO_2-8 wt.% Y_2O_3 ceramic layer was deposited on the bond coat surface via APS. Subsequently, a cyclic oxidation test was performed. Figures 9 and 10 display the results of this test for TBCs.

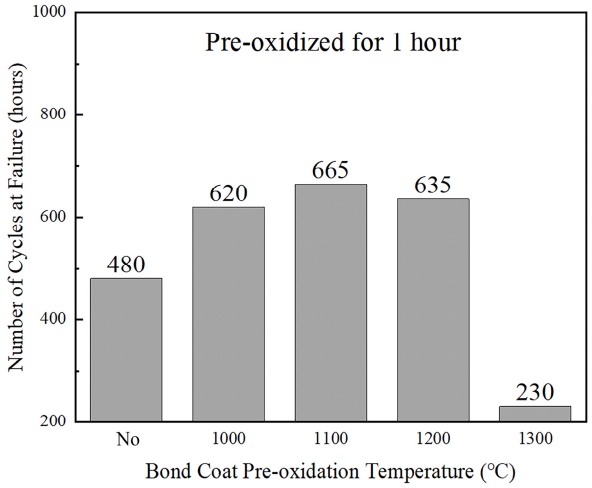

Figure 9. Effect of pre-heat-treatment temperature on cyclic oxidation life of TBCs [82].

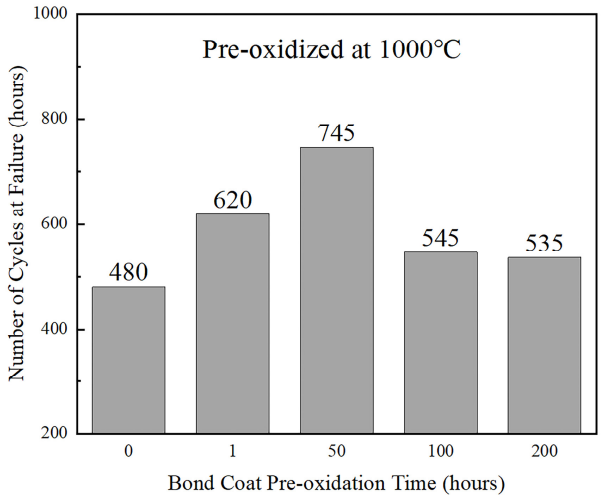

Figure 10. Effect of pre-heat-treatment time on cyclic oxidation life of TBCs [82].

After pre-heat-treatment at 1000, 1100 and 1200 °C for 1 h, a continuous and dense Al_2O_3 scale with a specific thickness was formed on the bond coat, leading to the TBC's thermal cycle life being significantly improved. However, the pre-heat-treatment at an excessively high temperature (1300 °C) produced mixed oxides on the bond coat surface, which greatly reduced the TBC's thermal cycle life (Figure 9).

The outcomes of the thermal cycle life analyses on the coatings with varied pre-heat-treatment times indicated that, for pre-heat-treatment periods less than 50 h, the oxidation resistance of the bond coat gradually elevated with an increase in duration. However, for coatings subjected to pre-heat-treatment periods greater than 50 h, their oxidation resistance and cycle life decreased significantly (Figure 10). This can be attributed to the formation of mixed oxides on the bond coat surface during the cyclic oxidation test, as a result of the depletion of the Al ions in the coatings due to the long pre-heat-treatment time.

6.2. The Effect of Pre-Heat-Treatment Oxygen Partial Pressure on Growth Behavior of TGO

Bi et al. [83] fabricated a NiCoCrAlY bond coat through EB-PVD. The as-deposited coatings underwent a pre-heat-treatment process in a low oxygen partial pressure environment at 1000 °C for 2 and 24 h, respectively, and were subsequently subjected to high temperature oxidation experiments in air at 1000 °C. The relationship between time and weight gain during the high temperature oxidation process of the coatings is illustrated in Figure 11. The oxidation weight gain rate of the bond coat subjected to pre-heat-treatment

is lower than that of the bond coat without pre-heat-treatment. Additionally, the bond coat pre-treated for 24 h exhibits a lower oxidation weight gain rate compared to the bond coat pre-treated for 2 h. This occurs due to the formation of the Al_2O_3 scale on the surface of the bond coat as a result of the pre-heat-treatment. Appropriate extension of the pre-heat-treatment time can increase the thickness of the oxide scale to a certain degree, thereby reducing the migration rate of ions in the oxide scale.

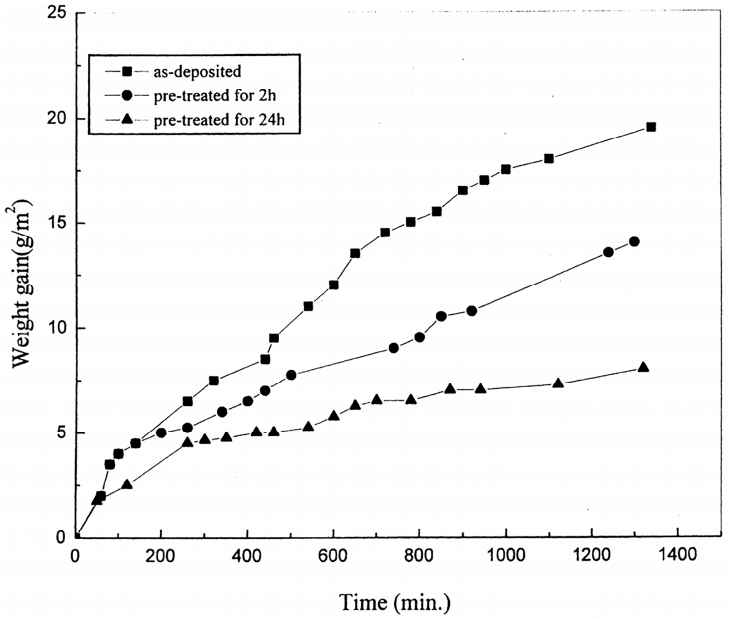

Figure 11. The relationship between weight gain and time of high temperature oxidation of an electron beam-physical vapor deposition (EB-PVD) NiCoCrAlY bond coat with different pre-treatments [83]. Copyright 2000, Elsevier.

Nijdam et al. [84] studied the effect of pre-oxidation oxygen partial pressure on the cyclic oxidation life of TBCs with a NiCoCrAlY bond coat prepared via high-speed physical-vapor deposition (HS-PVD). Figure 12 illustrates the outcomes of the cyclic oxidation test. It was observed that TBCs subjected to pre-oxidation with extremely low ($pO_2 = 1 \times 10^{-1}$ Pa) or high ($pO_2 = 2 \times 10^4$ Pa) oxygen partial pressure had a brief lifespan, while TBCs pre-oxidized at moderate oxygen partial pressure ($pO_2 = 1 \times 10^2$ Pa) displayed the longest lifetime.

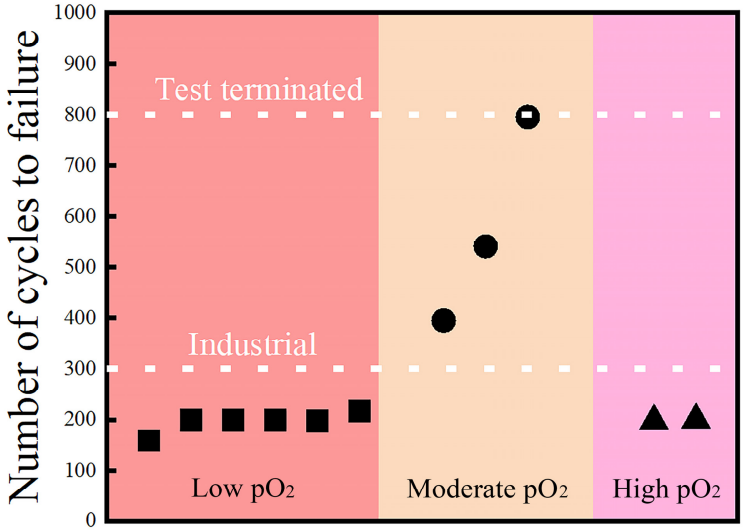

Figure 12. Effect of pre-oxidation oxygen partial pressure on TBCs cyclic oxidation life [84].

Matsumoto et al. [63] examined the impact of pre-heat-treatment oxygen partial pressure on the growth behavior of TGO on a VPS CoNiCrAlY bond coat, as well as on TBCs' cyclic oxidation life. The pre-heat-treatment oxygen partial pressure plays a crucial role in determining the structure of the oxide scale that is formed on the coating surface (Figure 13). Bond coats preheated with moderate oxygen partial pressure exhibit the lowest TGO thickness after 50 h of high-temperature oxidation (Figure 14a) and demonstrate the highest thermal cycle life during cyclic oxidation testing (Figure 14b). This is due to the fact that low-oxygen pre-heat-treatment fails to create a continuous Al_2O_3 scale, thus making it ineffective at providing adequate protection. In contrast, high-oxygen pre-heat-treatment leads to excessive aluminum consumption in the bond coat, causing premature formation of mixed oxides. On the other hand, moderate-oxygen pre-heat-treatment allows for the formation of a continuous, dense, and thin Al_2O_3 scale on the bond coat surface. This greatly reduces the growth rate of the TGO, ultimately extending the lifespan of TBCs.

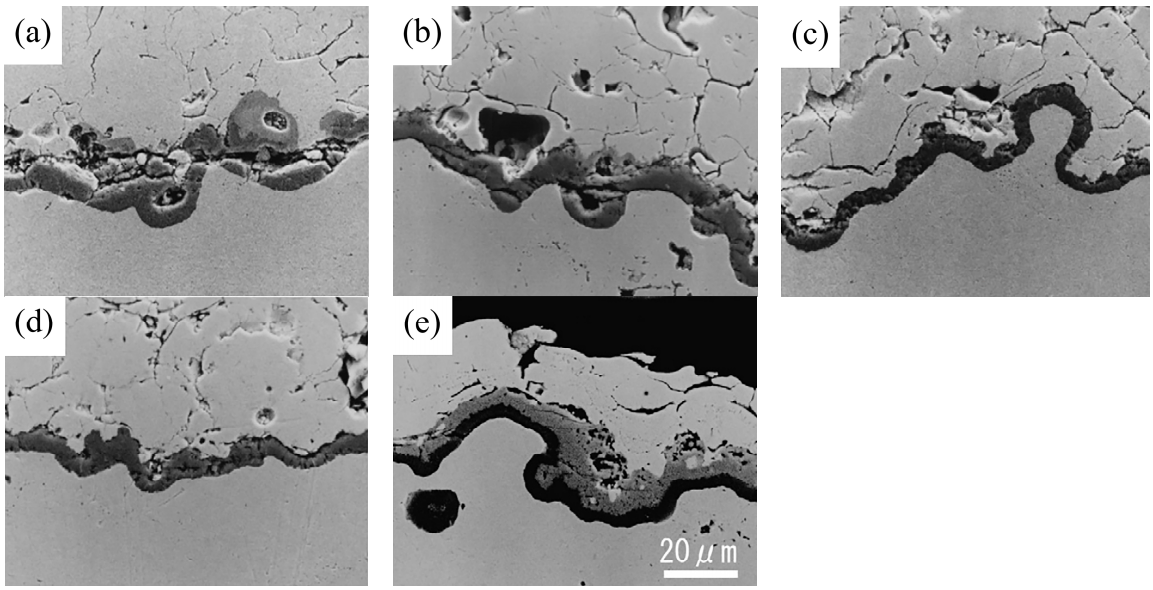

Figure 13. The cross-sectional structure of TGO in VPS CoNiCrAlY bond coats, which were pre-treated at different oxygen partial pressures, was observed after isothermal oxidation treatment at 1200 °C for 50 h in air. (**a**) $pO_2 = 2 \times 10^4$ Pa (in air), (**b**) $1 \times 10^{-7} \geq pO_2 \geq 1 \times 10^{-8}$ Pa, (**c**) $1 \times 10^{-9} \geq pO_2 \geq 1 \times 10^{-10}$ Pa, (**d**) $1 \times 10^{-11} \geq pO_2 \geq 1 \times 10^{-12}$ Pa, (**e**) without pre-heat-treatment [63]. Copyright 2006, Elsevier.

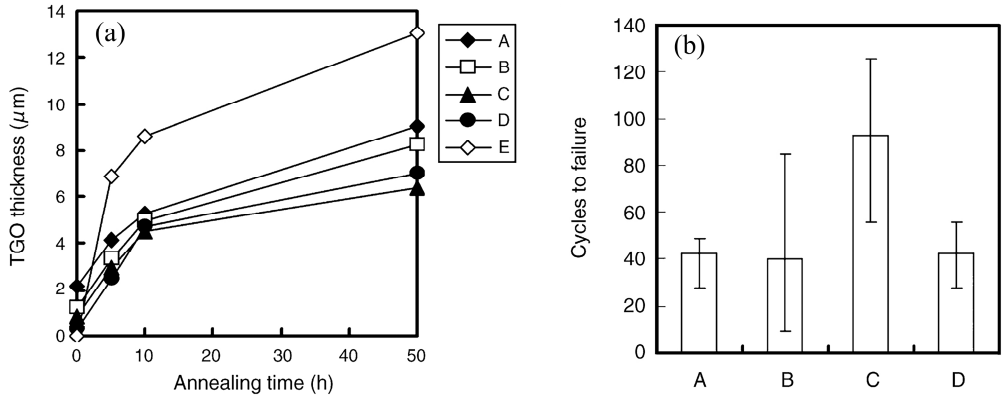

Figure 14. (**a**) Isothermal oxidation kinetics and (**b**) cyclic oxidation life of the VPS CoNiCrAlY bond coat with pre-heat-treatment at different oxygen partial pressures. A: $pO_2 = 2 \times 10^4$ Pa (in air); B: $1 \times 10^{-7} \geq pO_2 \geq 1 \times 10^{-8}$ Pa; C: $1 \times 10^{-9} \geq pO_2 \geq 1 \times 10^{-10}$ Pa; D: $1 \times 10^{-11} \geq pO_2 \geq 1 \times 10^{-12}$ Pa; E: without pre-heat-treatment [63]. Copyright 2006, Elsevier.

7. Summary and Prospect

This review provides a concise overview of MCrAlY bond coats, investigates the impact of bond coat microstructures and TGO growth behaviors on the bond coats' high-temperature oxidation resistance, and summarizes the effects of pre-heat-treatment on the high-temperature oxidation performance of the coating. The following conclusions have been drawn:

1. Appropriate pre-heat-treatment can reduce the porosity of the bond coat and facilitate the diffusion of Al element within the bond coat.
2. Appropriate pre-heat-treatment facilitates the formation of a continuous, dense, and moderately thick layer of pure Al_2O_3 TGO. This helps to delay the formation of mixed oxides and enhance the bond coats' oxidation resistance. It also allows for the control of TGO grain size, thereby reducing the growth rate of the TGO.
3. To achieve appropriate pre-heat-treatment, it is essential to carefully regulate the temperature to facilitate the formation of Al_2O_3, control the duration to ensure the uninterrupted growth of the Al_2O_3 scale while avoiding excessive aluminum depletion, and carefully manage the oxygen partial pressure to prevent the formation of mixed oxides.

To obtain a high-performance MCrAlY bond coat with outstanding oxidation resistance, it is recommended to employ raw powders with reduced oxygen content and utilize production methods in a low oxygen partial pressure environment. Furthermore, subject the bond coat to pre-heat-treatment under carefully controlled parameters, including temperatures within the range of 1000–1200 °C, durations lasting from 1 to 50 h, and oxygen partial pressures ranging from 1×10^{-10}–1×10^{2} Pa (the specific values should be selected according to the type of coating). Adhering to this approach will yield a bond coat displaying exceptional oxidation resistance throughout extended high-temperature operation periods.

The pre-treatment process of the bond coat is not about creating an oxide scale on the fresh metal surface, but rather involves the progressive growth and structural evolution of the initial oxide scale that is formed during bond coat preparation process. The structural evolution of the oxide scale significantly affects the growth behavior of TGO. To ensure superior performance and durability of bond coats, attention should be directed towards the entire process of bond coat preparation and pre-treatment. This would include fully considering aspects such as original powder preparation, bond coat preparation processes, pre-treatment processes, and other related factors in the development process. Such a comprehensive approach is essential to achieve bond coats that exhibit optimal performance and longevity.

Author Contributions: Conceptualization, B.Z., S.Z. and J.D.; methodology, B.Z., S.Z. and W.Y.; formal analysis, B.Z., J.D. and H.W.; investigation, B.Z., S.Z., J.D., W.Y., H.W. and G.L.; writing—original draft preparation, B.Z. and S.Z.; writing—review and editing, B.Z., S.Z., W.Y. and L.T.; visualization, B.Z., S.Z., J.D. and L.T.; supervision, B.Z., S.Z., H.W. and G.L. All authors have read and agreed to the published version of the manuscript.

Funding: This research was funded by Jiangxi Provincial Natural Science Foundation (Grant No.: 20212BAB214036) and the National Natural Science Foundation of China (Grant No.: 51901097).

Institutional Review Board Statement: Not applicable.

Informed Consent Statement: Not applicable.

Data Availability Statement: All data that support the findings of this study are included within the article.

Conflicts of Interest: The authors declare no conflict of interest.

References

1. Cheng, B.; Wei, Z.-Y.; Chen, L.; Yang, G.-J.; Li, C.-X.; Li, C.-J. Prolong the durability of La2Zr2O7/YSZ TBCs by decreasing the cracking driving force in ceramic coatings. *J. Eur. Ceram. Soc.* **2018**, *38*, 5482–5488. [CrossRef]
2. Zhang, W.-W.; Li, G.-R.; Zhang, Q.; Yang, G.-J. Multiscale pores in TBCs for lower thermal conductivity. *J. Therm. Spray Technol.* **2017**, *26*, 1183–1197. [CrossRef]
3. Zhang, W.-W.; Li, G.-R.; Zhang, Q.; Yang, G.-J.; Zhang, G.-W.; Mu, H.-M. Bimodal TBCs with low thermal conductivity deposited by a powder-suspension co-spray process. *J. Mater. Sci. Technol.* **2018**, *34*, 1293–1304. [CrossRef]
4. Zhang, W.-W.; Wei, Z.-Y.; Zhang, L.-Y.; Xing, Y.-Z.; Zhang, Q. Low-thermal-conductivity thermal barrier coatings with a multi-scale pore design and sintering resistance following thermal exposure. *Rare Met.* **2020**, *39*, 352–367. [CrossRef]
5. Liu, M.-J.; Yang, G.-J. Condensation behavior of gaseous phase during transported in the near-substrate boundary layer of plasma spray-physical vapor deposition. *J. Mater. Sci. Technol.* **2021**, *67*, 127–134. [CrossRef]
6. Cheng, B.; Yang, G.-J.; Zhang, Q.; Yang, N.; Zhang, M.; Zhang, Y.; Li, C.-X.; Li, C.-J. Gradient thermal cyclic behaviour of La2Zr2O7/YSZ DCL-TBCs with equivalent thermal insulation performance. *J. Eur. Ceram. Soc.* **2018**, *38*, 1888–1896. [CrossRef]
7. Sahoo, P.; Carr, T.; Martin, R.; Dinh, F. Thermal spray manufacturing issues in coating IGT hot section components. *J. Therm. Spray Technol.* **1998**, *7*, 481–483. [CrossRef]
8. Vardelle, A.; Moreau, C.; Akedo, J.; Ashrafizadeh, H.; Berndt, C.C.; Berghaus, J.O.; Boulos, M.; Brogan, J.; Bourtsalas, A.C.; Dolatabadi, A. The 2016 thermal spray roadmap. *J. Therm. Spray Technol.* **2016**, *25*, 1376–1440. [CrossRef]
9. Strangman, T.; Raybould, D.; Jameel, A.; Baker, W. Damage mechanisms, life prediction, and development of EB-PVD thermal barrier coatings for turbine airfoils. *Surf. Coat. Technol.* **2007**, *202*, 658–664. [CrossRef]
10. Zhang, Q.; Li, C.-J.; Li, Y.; Zhang, S.-L.; Wang, X.-R.; Yang, G.-J.; Li, C.-X. Thermal failure of nanostructured thermal barrier coatings with cold-sprayed nanostructured NiCrAlY bond coat. *J. Therm. Spray Technol.* **2008**, *17*, 838–845. [CrossRef]
11. Chen, L.; Yang, G.-J.; Li, C.-X.; Li, C.-J. Hierarchical formation of intrasplat cracks in thermal spray ceramic coatings. *J. Therm. Spray Technol.* **2016**, *25*, 959–970. [CrossRef]
12. Li, C.-J.; Li, Y.; Yang, G.-J.; Li, C.-X. A novel plasma-sprayed durable thermal barrier coating with a well-bonded YSZ interlayer between porous YSZ and bond coat. *J. Therm. Spray Technol.* **2012**, *21*, 383–390. [CrossRef]
13. Yang, D.; Gao, Y.; Liu, H.; Sun, C. Thermal shock resistance of bimodal structured thermal barrier coatings by atmospheric plasma spraying using nanostructured partially stabilized zirconia. *Surf. Coat. Technol.* **2017**, *315*, 9–16. [CrossRef]
14. Zhou, F.; Wang, Y.; Wang, L.; Cui, Z.; Zhang, Z. High temperature oxidation and insulation behavior of plasma-sprayed nanostructured thermal barrier coatings. *J. Alloys Compd.* **2017**, *704*, 614–623. [CrossRef]
15. Mauer, G.; Sebold, D.; Vaßen, R.; Hejrani, E.; Naumenko, D.; Quadakkers, W.J. Impact of processing conditions and feedstock characteristics on thermally sprayed MCrAlY bond coat properties. *Surf. Coat. Technol.* **2017**, *318*, 114–121. [CrossRef]
16. Fan, W.; Bai, Y.; Li, J.; Gao, Y.; Chen, H.; Kang, Y.; Shi, W.; Li, B. Microstructural design and properties of supersonic suspension plasma sprayed thermal barrier coatings. *J. Alloys Compd.* **2017**, *699*, 763–774. [CrossRef]
17. Wang, Y.; Bai, Y.; Liu, K.; Wang, J.; Kang, Y.; Li, J.; Chen, H.; Li, B. Microstructural evolution of plasma sprayed submicron-/nano-zirconia-based thermal barrier coatings. *Appl. Surf. Sci.* **2016**, *363*, 101–112. [CrossRef]
18. Tang, J.; Bai, Y.; Zhang, J.; Liu, K.; Liu, X.; Zhang, P.; Wang, Y.; Zhang, L.; Liang, G.; Gao, Y. Microstructural design and oxidation resistance of CoNiCrAlY alloy coatings in thermal barrier coating system. *J. Alloys Compd.* **2016**, *688*, 729–741. [CrossRef]
19. Padture, N.P.; Gell, M.; Jordan, E.H. Thermal barrier coatings for gas-turbine engine applications. *Science* **2002**, *296*, 280–284. [CrossRef]
20. Ouyang, T.; Wu, J.; Yasir, M.; Zhou, T.; Fang, X.; Wang, Y.; Liu, D.; Suo, J. Effect of TiC self-healing coatings on the cyclic oxidation resistance and lifetime of thermal barrier coatings. *J. Alloys Compd.* **2016**, *656*, 992–1003. [CrossRef]
21. Lv, B.; Xie, H.; Xu, R.; Fan, X.; Zhang, W.; Wang, T. Effects of sintering and mixed oxide growth on the interface cracking of air-plasma-sprayed thermal barrier coating system at high temperature. *Appl. Surf. Sci.* **2016**, *360*, 461–469. [CrossRef]
22. Chen, L.; Yang, G.-J.; Li, C.-X.; Li, C.-J. Edge effect on crack patterns in thermally sprayed ceramic splats. *J. Therm. Spray Technol.* **2016**, *26*, 302–314. [CrossRef]
23. Chen, L.; Yang, G.-J. Epitaxial growth and cracking of highly tough 7YSZ splats by thermal spray technology. *J. Adv. Ceram.* **2017**, *7*, 17–29. [CrossRef]
24. Li, G.; Yang, G. Understanding of degradation-resistant behavior of nanostructured thermal barrier coatings with bimodal structure. *J. Mater. Sci. Technol.* **2019**, *35*, 231–238. [CrossRef]
25. Cheng, B.; Yang, N.; Zhang, Q.; Zhang, M.; Zhang, Y.-M.; Chen, L.; Yang, G.-J.; Li, C.-X.; Li, C.-J. Sintering induced the failure behavior of dense vertically crack and lamellar structured TBCs with equivalent thermal insulation performance. *Ceram. Int.* **2017**, *43*, 15459–15465. [CrossRef]
26. Xie, H.; Xie, Y.-C.; Yang, G.-J.; Li, C.-X.; Li, C.-J. Modeling thermal conductivity of thermally sprayed coatings with intrasplat cracks. *J. Therm. Spray Technol.* **2013**, *22*, 1328–1336. [CrossRef]
27. Zhang, W.-W.; Li, G.-R.; Zhang, Q.; Yang, G.-J.; Zhang, G.-W.; Mu, H.-M. Self-enhancing thermal insulation performance of bimodal-structured thermal barrier coating. *J. Therm. Spray Technol.* **2018**, *27*, 1064–1075. [CrossRef]

28. Li, C.-J.; Li, Y.; Yang, G.-J.; Li, C.-X. Evolution of lamellar interface cracks during isothermal cyclic test of plasma-sprayed 8YSZ coating with a columnar-structured YSZ interlayer. *J. Therm. Spray Technol.* **2013**, *22*, 1374–1382. [CrossRef]
29. Dong, H.; Yang, G.-J.; Cai, H.-N.; Li, C.-X.; Li, C.-J. Propagation feature of cracks in plasma-sprayed YSZ coatings under gradient thermal cycling. *Ceram. Int.* **2015**, *41*, 3481–3489. [CrossRef]
30. He, J. Advanced MCrAlY alloys with doubled TBC lifetime. *Surf. Coat. Technol.* **2022**, *448*, 128931. [CrossRef]
31. Li, C.; Yuan, X.; Li, D.; Song, P.; Li, Z.; Huang, T.; Feng, J.; He, Y.; Zhai, R.; Li, Q. Test atmospheres affecting voids distribution on MCrAlY-bond coats for TBCs at 1050 °C. *Corros. Sci.* **2022**, *195*, 109967. [CrossRef]
32. Dong, H.; Yang, G.; Luo, X.; Li, C. Effects of mixed oxides on thermal cyclic lifetime of plasma-sprayed thermal barrier coatings. *China Surf. Eng.* **2015**, *28*, 21–28. [CrossRef]
33. Dong, H.; Yao, J.-T.; Li, X.; Zhou, Y.; Li, Y.-B. The sintering behavior of plasma-sprayed YSZ coating over the delamination crack in low temperature environment. *Ceram. Int.* **2018**, *44*, 3326–3332. [CrossRef]
34. Liu, T.; Yao, S.-W.; Wang, L.-S.; Yang, G.-J.; Li, C.-X.; Li, C.-J. Plasma-sprayed thermal barrier coatings with enhanced splat bonding for CMAS and corrosion protection. *J. Therm. Spray Technol.* **2015**, *25*, 213–221. [CrossRef]
35. Dong, L.; Liu, M.-J.; Zhang, X.-F.; Zhuo, X.-S.; Fan, J.-F.; Yang, G.-J.; Zhou, K.-S. Pressure infiltration of molten aluminum for densification of environmental barrier coatings. *J. Adv. Ceram.* **2021**, *11*, 145–157. [CrossRef]
36. Li, C.-J.; Dong, H.; Ding, H.; Yang, G.-J.; Li, C.-X. The correlation of the TBC lifetimes in burner cycling test with thermal gradient and furnace isothermal cycling test by TGO effects. *J. Therm. Spray Technol.* **2017**, *26*, 378–387. [CrossRef]
37. Liu, M.-J.; Zhang, M.; Zhang, Q.; Yang, G.-J.; Li, C.-X.; Li, C.-J. Evaporation of droplets in plasma spray–physical vapor deposition based on energy compensation between self-cooling and plasma heat transfer. *J. Therm. Spray Technol.* **2017**, *26*, 1641–1650. [CrossRef]
38. Chen, Q.-Y.; Peng, X.-Z.; Yang, G.-J.; Li, C.-X.; Li, C.-J. Characterization of plasma jet in plasma spray-physical vapor deposition of YSZ using a <80 kW shrouded torch based on optical emission spectroscopy. *J. Therm. Spray Technol.* **2015**, *24*, 1038–1045. [CrossRef]
39. Zhang, B.-Y.; Yang, G.-J.; Li, C.-X.; Li, C.-J. Non-parabolic isothermal oxidation kinetics of low pressure plasma sprayed MCrAlY bond coat. *Appl. Surf. Sci.* **2017**, *406*, 99–109. [CrossRef]
40. Meng, G.-H.; Liu, H.; Xu, P.-Y.; Li, G.-R.; Xu, T.; Yang, G.-J.; Li, C.-J. Superior oxidation resistant MCrAlY bond coats prepared by controlled atmosphere heat treatment. *Corros. Sci.* **2020**, *170*, 108653. [CrossRef]
41. Meng, G.-H.; Liu, H.; Liu, M.-J.; Xu, T.; Yang, G.-J.; Li, C.-X.; Li, C.-J. Large-grain α-Al_2O_3 enabling ultra-high oxidation-resistant MCrAlY bond coats by surface pre-agglomeration treatment. *Corros. Sci.* **2020**, *163*, 108275. [CrossRef]
42. Meng, G.-H.; Liu, H.; Liu, M.-J.; Xu, T.; Yang, G.-J.; Li, C.-X.; Li, C.-J. Highly oxidation resistant MCrAlY bond coats prepared by heat treatment under low oxygen content. *Surf. Coat. Technol.* **2019**, *368*, 192–201. [CrossRef]
43. Meng, G.-H.; Zhang, B.-Y.; Liu, H.; Yang, G.-J.; Xu, T.; Li, C.-X.; Li, C.-J. Highly oxidation resistant and cost effective MCrAlY bond coats prepared by controlled atmosphere heat treatment. *Surf. Coat. Technol.* **2018**, *347*, 54–65. [CrossRef]
44. Chen, H.; Fan, M.; Li, L.; Zhu, W.; Li, H.; Li, J.; Yin, Y. Effects of internal oxide contents on the oxidation and β-phase depletion behaviour in HOVF CoNiCrAlY coatings. *Surf. Coat. Technol.* **2021**, *424*, 127666. [CrossRef]
45. Ghadami, F.; Sabour Rouh Aghdam, A.; Ghadami, S. A comprehensive study on the microstructure evolution and oxidation resistance of conventional and nanocrystalline MCrAlY coatings. *Sci. Rep.* **2021**, *11*, 875. [CrossRef]
46. Mauer, G. Development of plasma parameters for the manufacture of MCrAlY bond coats by low-pressure plasma spraying using a cascaded torch. *Adv. Eng. Mater.* **2022**, *24*, 2200856. [CrossRef]
47. Ozgurluk, Y.; Karaoglanli, A.C.; Ahlatci, H. Comparison of calcium–magnesium-alumina-silicate (CMAS) resistance behavior of produced with electron beam physical vapor deposition (EB-PVD) method YSZ and $Gd_2Zr_2O_7$/YSZ thermal barrier coatings systems. *Vacuum* **2021**, *194*, 110576. [CrossRef]
48. Doleker, K.M.; Ozgurluk, Y.; Kahraman, Y.; Karaoglanli, A.C. Oxidation and hot corrosion resistance of HVOF/EB-PVD thermal barrier coating system. *Surf. Coat. Technol.* **2021**, *409*, 126862. [CrossRef]
49. Eriksson, R.; Yuan, K.; Li, X.-H.; Peng, R.L. MCrAlY coating design based on oxidation–diffusion modelling. Part II: Lifing aspects. *Surf. Coat. Technol.* **2014**, *253*, 27–37. [CrossRef]
50. Gil, A.; Shemet, V.; Vassen, R.; Subanovic, M.; Toscano, J.; Naumenko, D.; Singheiser, L.; Quadakkers, W. Effect of surface condition on the oxidation behaviour of MCrAlY coatings. *Surf. Coat. Technol.* **2006**, *201*, 3824–3828. [CrossRef]
51. Lau, H. Influence of yttria on the cyclic lifetime of YSZ TBC deposited on EB-PVD NiCoCrAlY bondcoats and its contribution to a modified TBC adhesion mechanism. *Surf. Coat. Technol.* **2013**, *235*, 121–126. [CrossRef]
52. Ren, C.; He, Y.; Wang, D. High-temperature cyclic oxidation behavior of Al_2O_3–YAG composite coating prepared by EPD and microwave sintering. *Appl. Surf. Sci.* **2012**, *258*, 5739–5745. [CrossRef]
53. Shuting, Z.; Donghai, G.; Hui, W.; Weiwei, W.; Yao, M. Research on the antioxidant property of MCrAlY alloy powders. *Rare Met. Mater. Eng.* **2014**, *43*, 2580–2583. [CrossRef]
54. Zhang, Q.; Li, C.-J.; Li, C.-X.; Yang, G.-J.; Lui, S.-C. Study of oxidation behavior of nanostructured NiCrAlY bond coatings deposited by cold spraying. *Surf. Coat. Technol.* **2008**, *202*, 3378–3384. [CrossRef]

55. Tang, F.; Ajdelsztajn, L.; Kim, G.E.; Provenzano, V.; Schoenung, J.M. Effects of surface oxidation during HVOF processing on the primary stage oxidation of a CoNiCrAlY coating. *Surf. Coat. Technol.* **2004**, *185*, 228–233. [CrossRef]
56. Tang, F.; Ajdelsztajn, L.; Schoenung, J.M. Influence of cryomilling on the morphology and composition of the oxide scales formed on HVOF CoNiCrAlY coatings. *Oxid. Met.* **2004**, *61*, 219–238. [CrossRef]
57. Kitaoka, S.; Kuroyama, T.; Matsumoto, M.; Kitazawa, R.; Kagawa, Y. Control of polymorphism in Al_2O_3 scale formed by oxidation of alumina-forming alloys. *Corros. Sci.* **2010**, *52*, 429–434. [CrossRef]
58. Choquet, P.; Mevrel, R. Microstructure of alumina scales formed on NiCoCrAl alloys with and without yttrium. *Mater. Sci. Eng. A* **1989**, *120*, 153–159. [CrossRef]
59. Iwamoto, H.; Sumikawa, T.; Nishida, K.; Asano, T.; Nishida, M.; Araki, T. High temperature oxidation behavior of laser clad NiCrAlY layer. *Mater. Sci. Eng. A* **1998**, *241*, 251–258. [CrossRef]
60. Tolpygo, V.; Clarke, D. Microstructural study of the theta-alpha transformation in alumina scales formed on nickel-aluminides. *Mater. High Temp.* **2000**, *17*, 59–70. [CrossRef]
61. Busso, E.; Lin, J.; Sakurai, S.; Nakayama, M. A mechanistic study of oxidation-induced degradation in a plasma-sprayed thermal barrier coating system.: Part I: Model formulation. *Acta Mater.* **2001**, *49*, 1515–1528. [CrossRef]
62. Maier, R.D.; Scheuermann, C.M.; Andrews, C.W. Degradation of a two-layer thermal barrier coating under thermal cycling. *Am. Ceram. Soc. Bull.* **1981**, *60*, 555–560.
63. Matsumoto, M.; Hayakawa, K.; Kitaoka, S.; Matsubara, H.; Takayama, H.; Kagiya, Y.; Sugita, Y. The effect of preoxidation atmosphere on oxidation behavior and thermal cycle life of thermal barrier coatings. *Mater. Sci. Eng. A* **2006**, *441*, 119–125. [CrossRef]
64. Teixeira, V.; Andritschky, M.; Fischer, W.; Buchkremer, H.; Stöver, D. Effects of deposition temperature and thermal cycling on residual stress state in zirconia-based thermal barrier coatings. *Surf. Coat. Technol.* **1999**, *120*, 103–111. [CrossRef]
65. Li, Y.; Li, C.-J.; Zhang, Q.; Yang, G.-J.; Li, C.-X. Influence of TGO composition on the thermal shock lifetime of thermal barrier coatings with cold-sprayed MCrAlY bond coat. *J. Therm. Spray Technol.* **2010**, *19*, 168–177. [CrossRef]
66. Xu, R.; Fan, X.L.; Zhang, W.X.; Wang, T. Interfacial fracture mechanism associated with mixed oxides growth in thermal barrier coating system. *Surf. Coat. Technol.* **2014**, *253*, 139–147. [CrossRef]
67. Dong, H.; Yang, G.J.; Li, C.X.; Luo, X.T.; Li, C.J. Effect of TGO thickness on thermal cyclic lifetime and failure mode of plasma-sprayed TBC s. *J. Am. Ceram. Soc.* **2014**, *97*, 1226–1232. [CrossRef]
68. Rabiei, A.; Evans, A. Failure mechanisms associated with the thermally grown oxide in plasma-sprayed thermal barrier coatings. *Acta Mater.* **2000**, *48*, 3963–3976. [CrossRef]
69. Evans, A.; He, M.; Hutchinson, J. Mechanics-based scaling laws for the durability of thermal barrier coatings. *Prog. Mater. Sci.* **2001**, *46*, 249–271. [CrossRef]
70. Yao, J.; He, Y.; Wang, D.; Peng, H.; Guo, H.; Gong, S. Thermal barrier coating bonded by (Al_2O_3–Y_2O_3)/(Y_2O_3-stabilized ZrO_2) laminated composite coating prepared by two-step cyclic spray pyrolysis. *Corros. Sci.* **2014**, *80*, 37–45. [CrossRef]
71. Ahrens, M.; Vaßen, R.; Stöver, D. Stress distributions in plasma-sprayed thermal barrier coatings as a function of interface roughness and oxide scale thickness. *Surf. Coat. Technol.* **2002**, *161*, 26–35. [CrossRef]
72. Li, Y.; Li, C.-J.; Yang, G.-J.; Xing, L.-K. Thermal fatigue behavior of thermal barrier coatings with the MCrAlY bond coats by cold spraying and low-pressure plasma spraying. *Surf. Coat. Technol.* **2010**, *205*, 2225–2233. [CrossRef]
73. Evans, A.G.; Mumm, D.; Hutchinson, J.; Meier, G.; Pettit, F. Mechanisms controlling the durability of thermal barrier coatings. *Prog. Mater. Sci.* **2001**, *46*, 505–553. [CrossRef]
74. Saeidi, S.; Voisey, K.T.; McCartney, D.G. The effect of heat treatment on the oxidation behavior of HVOF and VPS CoNiCrAlY coatings. *J. Therm. Spray Technol.* **2009**, *18*, 209–216. [CrossRef]
75. Ullah, A.; Khan, A.; Bao, Z.B.; Yu, C.T.; Zhu, S.L.; Wang, F.H. Effect of vacuum annealing on initial oxidation behavior and alumina transition of NiCoCrAlY coatings. *Surf. Coat. Technol.* **2020**, *404*, 126441. [CrossRef]
76. Yang, G.-J.; Xiang, X.-D.; Xing, L.-K.; Li, D.-J.; Li, C.-J.; Li, C.-X. Isothermal oxidation behavior of NiCoCrAlTaY coating deposited by high velocity air-fuel spraying. *J. Therm. Spray Technol.* **2012**, *21*, 391–399. [CrossRef]
77. Vande Put, A.; Oquab, D.; Péré, E.; Raffaitin, A.; Monceau, D. Beneficial effect of Pt and of pre-oxidation on the oxidation behaviour of an NiCoCrAlYTa bond-coating for thermal barrier coating systems. *Oxid. Met.* **2011**, *75*, 247–279. [CrossRef]
78. Swadźba, R.; Wiedermann, J.; Hetmańczyk, M.; Swadźba, L.; Witala, B.; Moskal, G.; Mendala, B.; Komendera, Ł. Microstructural examination of TGO formed during pre-oxidation on Pt-aluminized Ni-based superalloy. *Mater. Corros.* **2014**, *65*, 319–323. [CrossRef]
79. Swadźba, R. Interfacial phenomena and evolution of modified aluminide bond coatings in Thermal Barrier Coatings. *Appl. Surf. Sci.* **2018**, *445*, 133–144. [CrossRef]
80. Xie, S.F.; Zhang, L.W.; Ning, X.J.; Wang, L.; Lu, D.P. Effect of pre-oxidation on the isothermal and cyclic oxidation behaviour of cold-sprayed NiCoCrAlY coating. *Mater. Res. Innov.* **2015**, *19*, S9-258–S9-262. [CrossRef]
81. Zhang, B.-Y.; Shi, J.; Yang, G.-J.; Li, C.-X.; Li, C.-J. Healing of the interface between splashed particles and underlying bulk coating and its influence on isothermal oxidation behavior of LPPS MCrAlY bond coat. *J. Therm. Spray Technol.* **2015**, *24*, 611–621. [CrossRef]
82. Lih, W.; Chang, E.; Wu, B.; Chao, C. Effects of bond coat preoxidation on the properties of ZrO_2-8wt.% Y_2O_3/Ni-22Cr-10Al-1Y thermal-barrier coatings. *Oxid. Met.* **1991**, *36*, 221–238. [CrossRef]

83. Bi, X.; Xu, H.; Gong, S. Investigation of the failure mechanism of thermal barrier coatings prepared by electron beam physical vapor deposition. *Surf. Coat. Technol.* **2000**, *130*, 122–127. [CrossRef]
84. Nijdam, T.J.; Marijnissen, G.H.; Vergeldt, E.; Kloosterman, A.B.; Sloof, W.G. Development of a pre-oxidation treatment to improve the adhesion between thermal barrier coatings and NiCoCrAlY bond coatings. *Oxid. Met.* **2006**, *66*, 269–294. [CrossRef]